DOI:
10.1016/j.bmcl.2021.128044

Document Version
Version created as part of publication process; publisher's layout; not normally made publicly available

Journal Pre-proofs

Dipeptide Inhibitors of the Prostate Specific Membrane Antigen (PSMA): A Comparison of Urea and Thiourea Derivatives

Jennifer D Young, Michelle T Ma, Thomas R Eykyn, R. Andrew Atkinson, Vincenzo Abbate, Agostino Cilibrizzi, Robert C Hider, Philip J Blower

PII: S0960-894X(21)00270-5
DOI: https://doi.org/10.1016/j.bmcl.2021.128044
Reference: BMCL 128044

To appear in: *Bioorganic & Medicinal Chemistry Letters*

Received Date: 1 February 2021
Revised Date: 8 April 2021
Accepted Date: 11 April 2021

Please cite this article as: Young, J.D., Ma, M.T., Eykyn, T.R., Atkinson, R.A., Abbate, V., Cilibrizzi, A., Hider, R.C., Blower, P.J., Dipeptide Inhibitors of the Prostate Specific Membrane Antigen (PSMA): A Comparison of Urea and Thiourea Derivatives, *Bioorganic & Medicinal Chemistry Letters* (2021), doi: https://doi.org/10.1016/j.bmcl.2021.128044

Dipeptide Inhibitors of the Prostate Specific Membrane Antigen (PSMA): A Comparison of Urea and Thiourea Derivatives

Jennifer D Young[a], Michelle T Ma[a], Thomas R Eykyn[a], R. Andrew Atkinson[b], Vincenzo Abbate[c], Agostino Cilibrizzi[c], Robert C Hider[c], Philip J Blower[a]

a. School of Biomedical Engineering and Imaging Sciences, King's College London, London, United Kingdom

b. Centre for Biomolecular Spectroscopy and Randall Division of Cell and Molecular Biophysics, King's College London, London, United Kingdom

c. Institute of Pharmaceutical Science, King's College London, London, United Kingdom

Corresponding Author

Prof Philip J Blower. philip.blower@kcl.ac.uk

School of Biomedical Engineering and Imaging Sciences, 4th Floor, Lambeth Wing, St Thomas' Hospital, Westminster Bridge Road, London, SE17EH

Authors email addresses

jennifer.d.young@kcl.ac.uk

michelle.ma@kcl.ac.uk

thomas.eykyn@kcl.ac.uk

andrew.atkinson@ipbs.fr

vincenzo.abbate@kcl.ac.uk

agostino.cilibrizzi@kcl.ac.uk

robert.hider@kcl.ac.uk

philip.blower@kcl.ac.uk

Key Words

Glutamate carboxypeptidase II, GCP(II), prostate-specific membrane antigen, PSMA, prostate cancer, zinc(II) metalloenzyme, thiourea

Abstract

Glutamate carboxypeptidase II (GCP(II)), also known as the prostate-specific membrane antigen (PSMA), is a transmembrane zinc(II) metalloenzyme overexpressed in prostate cancer. Inhibitors of this receptor are used to target molecular imaging agents and molecular radiotherapy agents to prostate cancer and if the affinity of inhibitors for GCP(II)/PSMA was improved, targeting may also improve. Compounds containing the dipeptide OH-Lys-C(O)-Glu-OH (compound **3**), incorporating a urea motif, have high affinity for GCP(II)/PSMA. We hypothesized that substituting the zinc-coordinating urea group for a thiourea group, thus incorporating a sulfur atom, could facilitate stronger binding to zinc(II) within the active site, and thus improve affinity for GCP(II)/PSMA. A structurally analogous urea and thiourea pair (HO-Glu-C(O)-Glu-OH - compound **5** and HO-Glu-C(S)-Glu-OH - compound **6**) were synthesized and the inhibitory concentration (IC_{50}) of each compound

measured with a cell based assay, allowing us to refute the hypothesis: the thiourea analogue showed 100-fold weaker binding to PSMA than the urea analogue.

Graphical Abstract

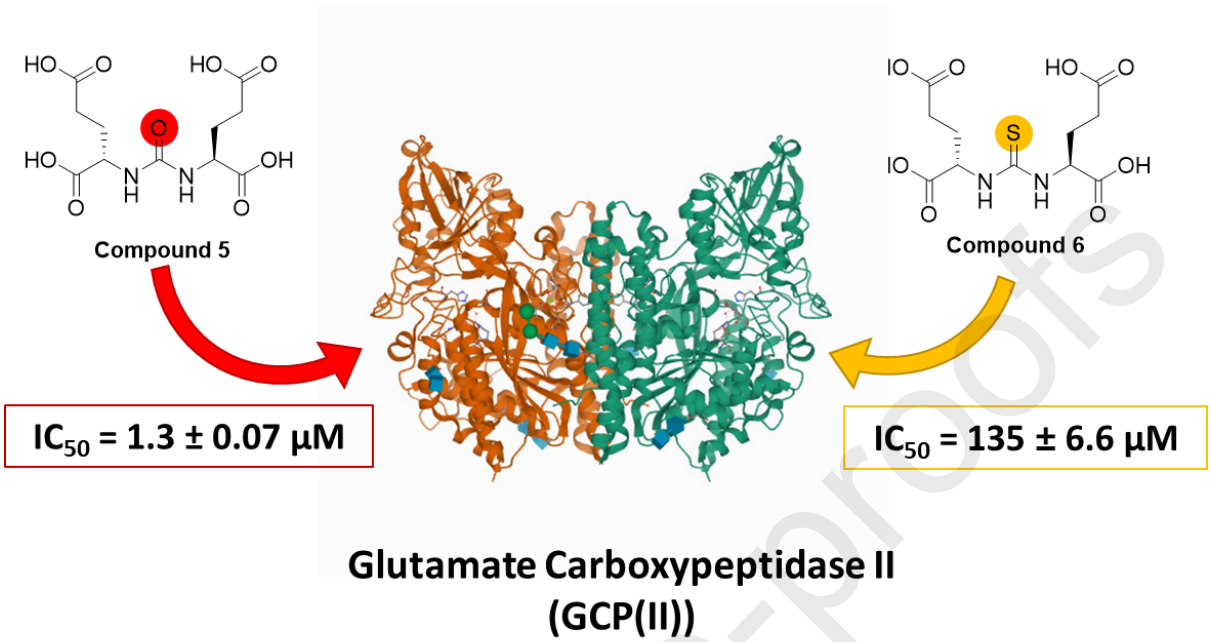

GCP II structure from protein data bank 2OOT (https://www.rcsb.org/structure/2OOT)

Main Article

In the last 5 years clinical management of prostate cancer has been transformed by the introduction of radiotracers targeting glutamate carboxypeptidase II (GCP(II)), also known as the prostate-specific membrane antigen (PSMA)[1,2,3,4]. Positron emission tomography/computed tomography (PET/CT) scans of prostate cancer patients imaged with radiotracers that target this receptor, such as [^{68}Ga]Ga-HBED-CC-PSMA[5] and [^{68}Ga]Ga-THP-PSMA[6], can provide clinically useful information about the location and spread of disease[1,2,3,4,7,8]. PET/CT scans allow clinicians to accurately stage patients and alter treatment plans accordingly[1,7]. Molecular radiotherapy with [^{177}Lu]Lu-PSMA-617 is currently being evaluated in a multinational phase 3 trial[9] (NCT NCT03511664). As a consequence, the demand for PSMA imaging agents is growing year on year. The excellent performance of these imaging agents is underpinned by two factors: i) GCP(II)/PSMA is very specific to prostate cancer, with 100-1000 fold higher expression in prostate cancer compared to normal prostate and low endogenous expression in other organs[10,11]; ii) radiotracers are designed to be very specific to GCP(II)/PSMA with K_i (equilibrium constant) and IC_{50} (half maximal inhibitory concentrations) values in the low nM to sub-nM range[5,6,12,13].

GCP(II)/PSMA is a transmembrane zinc(II) metalloenzyme that catalyzes the cleavage of terminal glutamates[14]. Its active site is specific for C-terminal glutamate residues, binding them tightly. A feature of the active site is the presence of two zinc(II) ions which participate in catalyzing the cleavage of the peptide bond between the terminal glutamate and the remainder of the substrate[15,16]. The natural substrates of GCP(II)/PSMA - N-Acetyl-L-aspartyl-L-glutamate (NAAG) and poly-glutamated-folates[14] - are shown in figure 1 (compounds **1** & **2** respectively). Examples of the dipeptide urea-based targeting motifs used in the majority of GCP(II)/PSMA targeted radiotracers[5,6,11,17,18] are also shown in figure 1. The OH-Lys-C(O)-Glu-OH (compound **3**) and OH-Cys-C(O)-Glu-OH (compound **4**) motifs were

developed by rational design from the natural substrates of GCP(II)/PSMA[19] and are remarkably small, simple and potent[5,12,17,18,19]. These ligands preserve the structure of the terminal glutamate but replace the peptide bond with a urea bond, thus reducing the electrophilicity of the carbonyl carbon atom and providing stability against enzymatic cleavage by GCP(II)/PSMA. The urea functional group links the glutamate to a second amino acid (L-lysine or L-cysteine), which can be used to functionalize this inhibitory motif[15]. For example, it can be converted into a PET radiotracer by adding a prosthetic group containing covalently-bound radionuclide such as fluorine-18[21,22], or a chelator allowing radiometals, such as gallium-68, to be incorporated[5,6,18,22].

Despite the success of the dipeptide urea-based motif and its proven utility in the clinic, it is expected that further improvement in affinity for GCP(II)/PSMA is possible. Valuable information to guide rational design is now available from X-ray crystallography studies[23,24,25], including evidence that the urea oxygen coordinates to Zn(II) in the active site[26], and many structural modifications to improve affinity have been attempted previously[12,16]. The main conclusions from this body of published work are: (i) the conservation of the terminal glutamate is extremely important and any modifications to it reduce affinity[12,16]; (ii) the ability of an inhibitor to bind the zinc(II) atoms in the active site also determines affinity[16]. Urea groups[19,25,26], phosphonates[13,25], phosphinates[13,25] and phosphonamidates[25,27] have been shown to bind strongly to zinc within GCP(II)/PSMA, with the urea closely mimicking the structure of a peptide bond and the others mimicking the tetrahedral transition state/intermediate (with an sp^3 hybridized carbon) during peptide bond cleavage[15]. This shows that the zinc(II)-binding group is amenable to variation and provides an opportunity to improve affinity (by enhancing Zn-binding) through modification of this group. It is also important that the selected zinc-binding group is resistant to enzymatic cleavage by GCP(II)/PSMA and that it can link the terminal glutamate to the rest of the inhibitor, which is used for functionalization.

The presence of zinc(II) ions in the active site has previously prompted investigators to look to thiols as zinc-binding motifs in GCP(II)/PSMA inhibitors, with limited success[28]. However, to date thiourea-based inhibitors have not been tested as GCP(II)/PSMA ligands. The rationale for replacing oxygen with sulfur in an inhibitor for a zinc(II)-based metalloenzyme is twofold. First, zinc(II) ions and sulfur-based ligands, including thiourea, have a strong affinity for each other and typically form highly stable complexes[29,30]. Zinc(II)-sulfur interactions are ubiquitous in biology, including functional processes (for example heat shock protein Hsp33 in which zinc(II) binds to redox-active thiolate groups that induce a conformation change upon oxidation[31]), and stabilization of structures (for example zinc(II) finger motifs that are common to many proteins[32]). Second, the resonance within the thiourea group favours more negative charge on the sulfur compared to the oxygen of the urea group; this would be expected to allow stronger interaction with the zinc(II) ions. We therefore hypothesized that replacing the urea with a thiourea in this class of dipeptide inhibitors could improve affinity.

To test this hypothesis, we elected to modify the symmetrical urea-based inhibitor compound **5** (HO-Glu-C(O)-Glu-OH), which is reported to have a K_i = 8 nM for GCP(II)/PSMA[12]. The thiourea analog compound **6** (HO-Glu-C(S)-Glu-OH), was designed to conserve the interactions in the glutamate binding pocket and remain resistant to enzymatic cleavage, but to have enhanced interactions with the zinc(II) ions through the presence of the sulfur atom. The formation of thiourea is synthetically achievable through an isothiocyanate intermediate, using existing well-characterized chemistry[33].

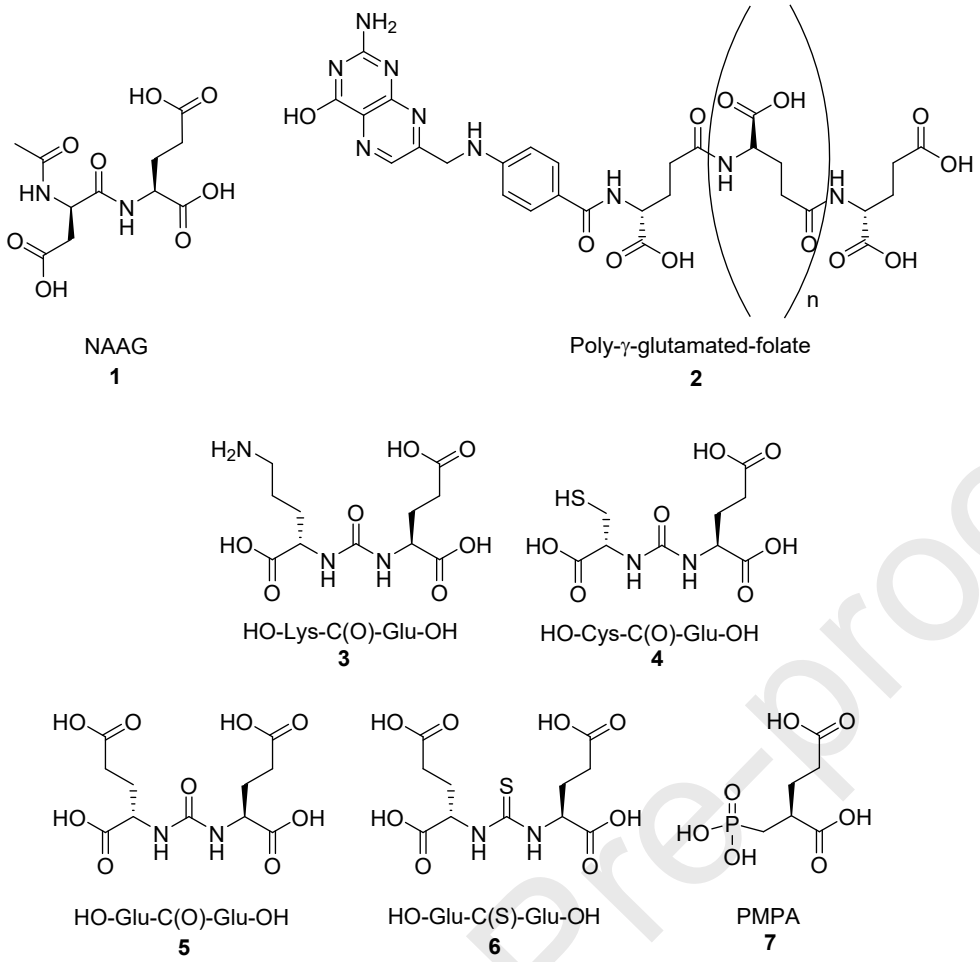

Figure 1: Structures of the natural substrates of GCP(II)/PSMA (top row) and known inhibitors and the novel inhibitor (compound **6** - HO-Glu-C(S)-Glu-OH) addressed in this communication.

Compounds **5** and **6** were synthesized by similar two-step synthetic routes. The reaction schemes for compound **5** are found in the supplemental files and the reaction scheme for compound **6** are found in figure 2. The first step was the formation of a urea or thiourea linkage between two t-butyl-protected L-glutamate residues (compound **8**). For the urea compound **14** ($Glu(tBu)_2$-C(O)-$Glu(tBu)_2$) a, triphosgene was used to generate an isocyanate intermediate, followed by reaction with another equivalent of compound **8**, to yield the desired product. For the thiourea compound **10** ($Glu(tBu)_2$-C(S)-$Glu(tBu)_2$), thiophosgene was used to generate an isothiocyanate intermediate with subsequent formation of a thiourea bond.

The second synthetic step removed the t-butyl protecting groups before purification of the final compounds. Compound **14** was deprotected using trifluoroacetic acid in the presence of phenol and triisopropylsilane as scavengers, and then isolated using semi-preparative reverse phase HPLC purification. However, when compound **10** was similarly deprotected using trifluoroacetic acid/ phenol/ triisopropylsilane, the major species obtained was compound **11** which contained a γ-lactam pyroglutamic acid residue. Similar cyclization reactions are well-known[34] and many peptides and proteins naturally have a pyroglutamic acid at their N terminus[35]. This suggests that compound **10** is more prone than compound **14** to dehydration under these conditions. This is likely to be due to the

stronger preference of thiourea for the enol/enolate resonance form, due to sulfur's weaker π-bonding and its concomitant ability to stabilize the negative charge.

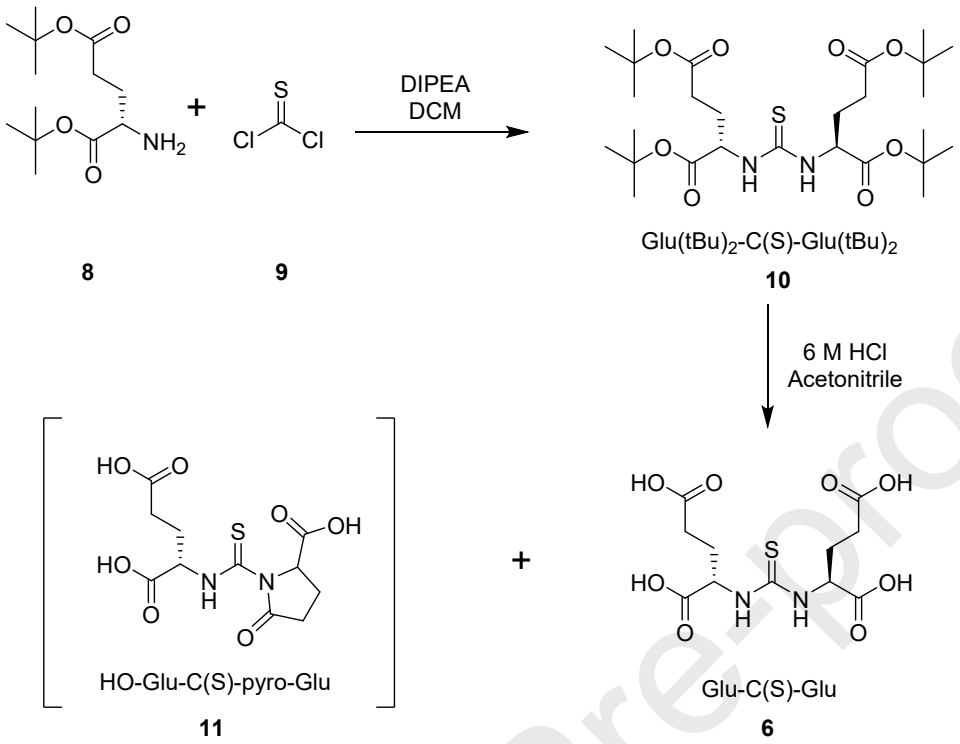

Figure 2: Synthesis route for the production of compound **6** (HO-Glu-C(S)-Glu-OH) and cyclized side product compound **11** (HO-Glu-C(S)-pyroGlu).

As cyclisation was particularly prevalent in high acid, low water conditions, the reaction conditions were modified to avoid it: compound **10** was reacted in a 2:1 solution of 6 M HCl and acetonitrile for 8 hours, followed by neutralization and purification by semi-preparative HPLC. This increased yields of compound **6**. Compounds **5** and **6** were characterized by nuclear magnetic resonance (NMR) and high-resolution mass spectrometry (supplemental files).

To ensure that compound **6** was resistant to cyclisation under conditions required for *in vitro* affinity measurements, NMR studies were conducted. Aqueous solutions of compound **5** and compound **6** at pH 7 (pH adjusted with phosphate-buffered saline (PBS) and ammonium acetate) were monitored using ^{1}H NMR (400 MHz) for 48 hours. Both inhibitors were stable, with no cyclisation detected under these conditions. ^{1}H NMR (400 MHz) was also used to monitor the stability of compound **6** with respect to cyclisation in the presence of GCP(II)/PSMA-expressing cells (DU145-PSMA); the thiourea ligand was found to be stable in these conditions.

Inhibition assays (IC_{50} assays) were conducted in triplicate to compare compound **7** (2-(phosphonomethyl)pentanedioic acid, (PMPA)), compound **5** and compound **6** over a concentration range of 1 nM to 400 µM. Compound **7** is a widely-used PSMA inhibitor that has a phosphonate zinc(II)-binding group (K_i = 0.3 nM[13]), and was included as an additional control. These competitive binding studies utilized GCP(II)/PSMA-expressing cells (DU145-PSMA[35]) and the radiolabeled PSMA imaging agent [^{67}Ga]Ga-DOTA-PSMA(617)[6,37] as the probe (1 nM DOTA-PSMA(617)). Non-GCP(II)/PSMA-expressing cells (DU145[36]) were used as a control to account for non-specific binding. The IC_{50} assays

revealed large differences in affinity between the three inhibitors (figure 3): compound **7** 94 ± 4 nM, compound **5** 1340 ± 70 nM, and compound **6** 135000± 6600 nM. **Table 1** shows the relative IC_{50} ratios for the three inhibitors. K_i values from isolated enzyme assays have been previously reported for compound **7** and compound **5**. The relative K_i ratio for these compounds match well with the relative IC_{50} ratio determined for the same inhibitors using our cell-based assay. A summary of the relationship between IC_{50} and K_i and when their relative ratios can be directly compared[38] is available in supplemental files.

The 100-fold increase in the IC_{50} value for the newly synthesized thiourea compared to the urea compound shows that the compound **6** is a much less potent inhibitor than compound **5**, and therefore this modification worsens rather than improves affinity – the opposite of our hypothesis. The quantification and stability tests performed confirmed that compound **6** was at the required concentration during the assay (supplemental files) and that it was stable for its duration. Therefore, this value is a true reflection of the change in IC_{50} value resulting from the replacement of urea with thiourea.

	PMPA Compound **7**	**HO-Glu-C(O)-Glu-OH** Compound **5**	**HO-Glu-C(S)-Glu-OH** Compound **6**
K_i (literature values)	0.3 nM [13]	8 nM [12]	-
IC_{50} (experimental values)	94 ± 4 nM	1340 ± 70 nM	135000± 6600 nM
Relative K_i ratio	Compound **5** K_i / Compound **7** K_i		Ratio 26.6
Relative IC_{50} ratio	Compound **5** IC_{50} / Compound **7** IC_{50}		Ratio 14.2
Relative IC_{50} ratio	Compound **6** IC_{50} / Compound **7** IC_{50}		Ratio 1436
Relative IC_{50} ratio	Compound **6** IC_{50} / Compound **5** IC_{50}		Ratio 101

Table 1: Literature K_i values [12,13] and experimental IC_{50} values for the inhibitors and the relative K_i ratios and relative IC_{50} ratios that used to compare the affinity of the inhibitors.

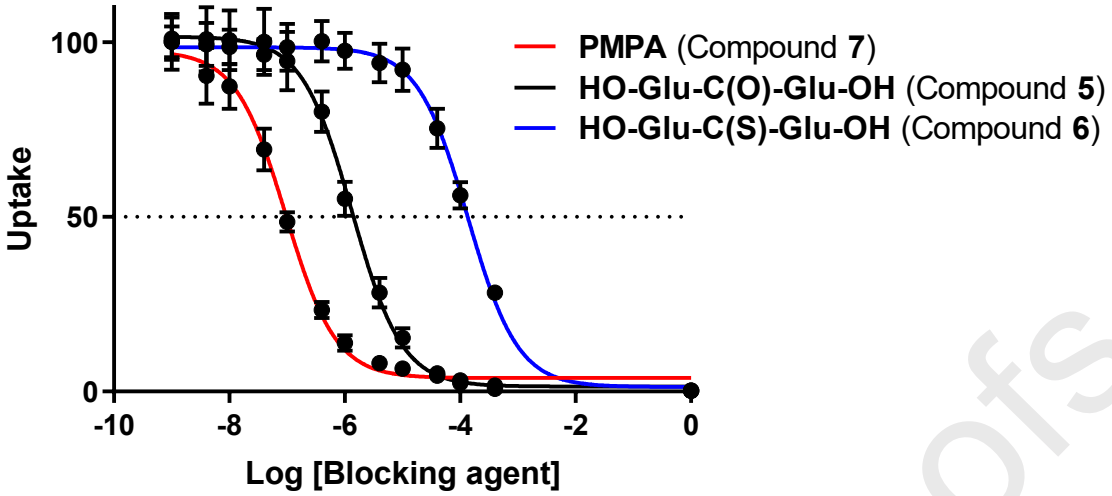

Figure 3: Inhibition curves for compounds **5, 6** and **7**, (HO-Glu-C(O)-Glu-OH, HO-Glu-C(S)-Glu-OH and PMPA) with [^{67}Ga]Ga-DOTA-PSMA at 1 nM as the probe. Values are averaged across triplicate assays. For each assay n = 4 wells at each concentration. Note that non-specific binding of [^{67}Ga]Ga-DOTA-PSMA with non-GCP(II)PSMA-expressing cells (DU145) was used as the nominal value at 1 M inhibitor.

Request for Figure 3 to be printed in color.

The unexpected low affinity of compound **6** could be due to the longer C=S bond relative to the C=O bond (1.71 Å[39] and 1.26 Å[40] respectively). Additionally, Zn-S bonds are also typically longer than Zn-O bonds[41]. Such changes could detrimentally perturb the interactions of other key functional inhibitor groups within the active site; the additive enthalpic cost of these weakened interactions may counteract any gain in affinity caused by the stronger bond between the zinc(II) ion and the thiourea sulfur atom. This is consistent with previous findings, which suggest that the effectiveness of a zinc(II) ion binding group for GCP(II)/PSMA ligands is dependent on maintaining the glutamate interactions within the active site[16].

This work expands existing knowledge about GCP(II)/PSMA and inhibitor design. Although the thiourea modification weakened affinity for the receptor, further investigation into novel ways to improve the affinity would be extremely valuable and could impact prostate cancer management.

Funding

JDY was funded by the King's College London and Imperial College London EPSRC Centre for Doctoral Training in Medical Imaging (EP/L015226/1) and Theragnostics Limited. AC was funded by Theragnostics Ltd. We acknowledge financial support from: King's Health Partners R&D Challenge Fund (MRC Confidence in concept (MC_PC_17164)); the Centre of Excellence in Medical Engineering funded by the Wellcome Trust and EPSRC (WT 088641/Z/09/Z); KCL and UCL Comprehensive Cancer Imaging Centre funded by CRUK and EPSRC in association with the MRC and DoH (England); EPSRC Programme Grant [#EP/S032789/1]; and the NIHR Biomedical Research Centre award to Guy's and St Thomas' NHS Foundation Trust in partnership with King's College London and King's College Hospital NHS Foundation Trust. The views expressed are those of the authors and not necessarily those of the NHS, NIHR or DoH. The NMR Facility at King's College London was enabled by grants from Wellcome and the British Heart Foundation.

Competing interests

The authors have no completing interests to declare.

References

1. Kulkarni M, Hughes S, Mallia A, et al. The management impact of 68gallium-tris(hydroxypyridinone) prostate-specific membrane antigen (68Ga-THP-PSMA) PET-CT imaging for high-risk and biochemically recurrent prostate cancer. *Eur J Nucl Med Mol Imaging*. 2020;47(3):674-686. doi:10.1007/s00259-019-04643-7

2. Müller J, Ferraro DA, Muehlematter UJ, et al. Clinical impact of 68 Ga-PSMA-11 PET on patient management and outcome, including all patients referred for an increase in PSA level during the first year after its clinical introduction. *Eur J Nucl Med Mol Imaging*. 2019;46(4):889-900. doi:10.1007/s00259-018-4203-0

3. Afaq A, Alahmed S, Chen S, et al. 68 Ga-PSMA PET/CT impact on prostate cancer management. *J Nucl Med*. 2018;59:89-92. doi:10.2967/jnumed.117.192625

4. Roach PJ, Francis R, Emmett L, et al. The impact of 68 Ga-PSMA PET/CT on management intent in prostate cancer: results of an Australian prospective multicenter study. *J Nucl Med*. 2018;59(1):82-88. doi:10.2967/jnumed.117.197160

5. Eder M, Schäfer M, Bauder-Wüst U, et al. 68Ga-complex lipophilicity and the targeting property of a urea-based PSMA inhibitor for PET imaging. *Bioconjug Chem*. 2012;23(4):688-697. doi:10.1021/bc200279b

6. Young JD, Abbate V, Imberti C, et al. 68Ga-THP-PSMA: a PET imaging agent for prostate cancer offering rapid, room-temperature, 1-step kit-based radiolabeling. *J Nucl Med*. 2017;58(8):1270-1277. doi:10.2967/jnumed.117.191882

7. Hofman MS, Eu P, Jackson P, et al. Cold kit PSMA PET imaging: phase I study of 68Ga-THP-PSMA PET/CT in patients with prostate cancer. *J Nucl Med*. 2018;59:625-631. doi:10.2967/jnumed.117.199554

8. Hofman MS, Lawrentschuk N, Francis RJ, et al. Prostate-specific membrane antigen PET-CT in patients with high-risk prostate cancer before curative-intent surgery or radiotherapy (proPSMA): a prospective, randomised, multi-centre study. *Lancet*. 2020;6736(20):1-9. doi:10.1016/s0140-6736(20)30314-7

9. Rahbar K, Bodei L, Morris MJ. Is the vision of radioligand therapy for prostate cancer becoming a reality? An overview of the phase III VISION trial and its importance for the future of theranostics. *J Nucl Med*. 2019;60(11):1504-1506. doi:10.2967/jnumed.119.234054

10. Ghosh A, Heston WDW. Tumor target prostate specific membrane antigen (PSMA) and its regulation in prostate cancer. *J Cell Biochem*. 2004;91(3):528-539. doi:10.1002/jcb.10661

11. O'Keefe DS, Bacich DJ, Heston WDW. Comparative analysis of prostate-specific membrane antigen (PSMA) versus a prostate-specific membrane antigen-like gene. *Prostate*. 2004;58:200-210. doi:10.1002/pros.10319

12. Kozikowski AP, Zhang J, Nan F, et al. Synthesis of urea-based inhibitors as active site probes of glutamate carboxypeptidase II: efficacy as analgesic agents. *J Med Chem*. 2004;47(7):1729-1738. doi:10.1021/jm0306226

13. Jackson PF, Slusher BS. Design of NAALADase inhibitors: a novel neuroprotective strategy. *CurrMedChem*. 2001;8(8):949-957. doi:10.2174/0929867013372797

14. Zhou J, Neale JH, Pomper MG, Kozikowski AP. NAAG peptidase inhibitors and their potential for diagnosis and therapy. *Nat Rev Drug Discov*. 2005;4(12):1015-1026. doi:10.1038/nrd1903

15. Klusák V, Bařinka C, Plechanovová A, et al. Reaction mechanism of glutamate carboxypeptidase II revealed by mutagenesis, X-ray crystallography, and computational methods. *Biochemistry*. 2009;48(19):4126-4138. doi:10.1021/bi900220s

16. Pavlicek J, Ptacek J, Barinka C. Glutamate carboxypeptidase II: an overview of structural studies and their importance for structure-based drug design and deciphering the reaction mechanism of the enzyme. *Curr Med Chem*. 2012;19(9):1300-1309. doi:CDT-EPUB-20120203-004 [pii]

17. Pomper MG, Musachio JL, Zhang J, et al. 11C-MCG: synthesis, uptake selectivity, and primate PET of a probe for glutamate carboxypeptidase II (NAALADase). *Mol Imaging*. 2002;1(2):96-101. doi:10.1162/153535002320162750

18. Wüstemann T, Bauder-Wüst U, Schäfer M, et al. Design of internalizing PSMA-specific glu-ureido-based radiotherapeuticals. *Theranostics*. 2016;6(8):1085-1095. doi:10.7150/thno.13448

19. Kozikowski AP, Nan F, Conti P, et al. Design of remarkably simple, yet potent urea-based inhibitors of glutamate carboxypeptidase II (NAALADase). *J Med Chem*. 2001;44(3):298-301. doi:10.1021/jm000406m

20. Chen Y, Pullambhatla M, Foss CA, et al. 2-(3-{1-carboxy-5-[(6-[18F]fluoro-pyridine-3-carbonyl)-amino]- pentyl}-ureido)-pentanedioic acid, [18F]DCFPyL, a PSMA-based PET imaging agent for prostate cancer. *Clin Cancer Res*. 2011;17(24):7645-7653. doi:10.1158/1078-0432.CCR-11-1357

21. Giesel FL, Hadaschik B, Cardinale J, et al. F-18 labelled PSMA-1007: biodistribution, radiation dosimetry and histopathological validation of tumor lesions in prostate cancer patients. *Eur J Nucl Med Mol Imaging*. 2017;44(4):678-688. doi:10.1007/s00259-016-3573-4

22. Kularatne SA, Zhou Z, Yang J, Post CB, Low PS. Design, synthesis, and preclinical evaluation of prostate-specific membrane antigen targeted 99mTc-radioimaging agents. *Mol Pharm*. 2009;6(3):790-800. doi:10.1021/mp9000712

23. Barinka C, Starkova J, Konvalinka J, Lubkowski J. A high-resolution structure of ligand-free human glutamate carboxypeptidase II. *Acta Crystallogr Sect F Struct Biol Cryst Commun*. 2007;63(3):150-153. doi:10.1107/S174430910700379X

24. Hlouchova K, Barinka C, Konvalinka J, Lubkowski J. Structural insight into the evolutionary and pharmacologic homology of glutamate carboxypeptidases II and III. *FEBS J*. 2009;276(16):4448-4462. doi:10.1111/j.1742-4658.2009.07152.x

25. Novakova Z, Cerny J, Choy CJ, et al. Design of composite inhibitors targeting glutamate carboxypeptidase II: the importance of effector functionalities. *FEBS J*. 2016;283(1):130-143. doi:10.1111/febs.13557

26. Barinka C, Byun Y, Dusich CL, et al. Interactions between human glutamate carboxypeptidase II and urea-based inhibitors: structural characterization. *J Med Chem*. 2008;51(24):7737-7743. doi:10.1021/jm800765e

27. Wu LY, Anderson MO, Toriyabe Y, et al. The molecular pruning of a phosphoramidate peptidomimetic inhibitor of prostate-specific membrane antigen. *Bioorganic Med Chem*. 2007;15(23):7434-7443. doi:10.1016/j.bmc.2007.07.028

28. Majer P, Jackson PF, Delahanty G, et al. Synthesis and biological evaluation of thiol-based

inhibitors of glutamate carboxypeptidase II : discovery of an orally active GCP II inhibitor. *J Med Chem*. 2003;46:1989-1996. doi:10.1021/jm020515w

29. Krężel A, Maret W. The biological inorganic chemistry of zinc ions. *Arch Biochem Biophys*. 2016;611:3-19. doi:10.1016/j.abb.2016.04.010

30. Dhumane NR, Hussaini SS, Dongre VG, Shirsat MD. Influence of glycine on the nonlinear optical (NLO) properties of zinc (tris) thiourea sulfate (ZTS) single crystal. *Opt Mater (Amst)*. 2008;31(2):328-332. doi:10.1016/j.optmat.2008.05.002

31. Jakob U, Eser M, Bardwell JCA. Redox switch of Hsp33 has a novel zinc-binding motif. *J Biol Chem*. 2000;275(49):38302-38310. doi:10.1074/jbc.M005957200

32. Klug A, Schwabe J. Zinc Fingers. *FASEB J*. 1995;9(8):597-604. doi:10.1096/fasebj.9.8.7768350

33. Maddani MR, Prabhu KR. A concise synthesis of substituted thiourea derivatives in aqueous medium. *J Org Chem*. 2010;75(7):2327-2332. doi:10.1021/jo1001593

34. Haitinger L. Vorläufige mittheilung über glutaminsäure und pyrrol. *Monatshefte für Chemie und verwandte Teile anderer Wissenschaften*. 1882;3:228–229.

35. Kumar A, Bachhawat AK. Pyroglutamic acid: throwing light on a lightly studied metabolite. *Curr Sci*. 2012;102(2):288-297. doi:10.2307/24083854

36. Kampmeier F, Williams JD, Maher J, Mullen GE, Blower PJ. Design and preclinical evaluation of a 99mTc-labelled diabody of mAb J591 for SPECT imaging of prostate-specific membrane antigen (PSMA). *EJNMMI Res*. 2014;4(1):13. doi:10.1186/2191-219X-4-13

37. Benešová M, Schäfer M, Bauder-Wüst U, et al. Preclinical evaluation of a tailor-made DOTA-conjugated PSMA inhibitor with optimized linker moiety for imaging and endoradiotherapy of prostate cancer. *J Nucl Med*. 2015;56:914-920. doi:10.2967/jnumed.114.147413

38. Kalliokoski T, Kramer C, Vulpetti A, Gedeck P. Comparability of Mixed IC50 Data - A Statistical Analysis. *PLoS One*. 2013;8(4). doi:10.1371/journal.pone.0061007

39. Kunchur NR, Truter MR. A detailed refinement of the crystal and molecular structure of thiourea. *J Chem Soc*. 1958;(0):2551-2557. doi:10.1039/JR9580002551

40. Vaughn P, Donahue J. The structure of urea. Interatomic distances and resonance in urea and related compounds. *Acta Crystallogr*. 1952;(5):530-535. doi:10.1107/S0365110X52001477

41. Tamames B, Sousa SF, Tamames J, Fernandes PA, Ramos MJ. Analysis of zinc-ligand bond lengths in metalloproteins: Trends and patterns. *Proteins*. 2007;69(3):466-475. doi:https://doi.org/10.1002/prot.21536

Supplemental Files

Dipeptide Inhibitors of the Prostate Specific Membrane Antigen (PSMA): A Comparison of Urea and Thiourea Derivatives

Jennifer D Young[a], Michelle T Ma[a], Thomas R Eykyn[a], R. Andrew Atkinson[b], Vincenzo Abbate[c], Agostino Cilibrizzi[c], Robert C Hider[c], Philip J Blower[a]

a. School of Biomedical Engineering and Imaging Sciences, King's College London, London, United Kingdom

b. Centre for Biomolecular Spectroscopy and Randall Division of Cell and Molecular Biophysics, King's College London, London, United Kingdom

c. Institute of Pharmaceutical Science, King's College London, London, United Kingdom

Instrumentation

Nuclear Magnetic Resonance (NMR): ^{1}H- and ^{13}C-NMR spectra were acquired on either a Bruker Avance III 400 spectrometer operating at 400 MHz (^{1}H frequency) equipped with a BBO probe, or a Bruker NEO 800 spectrometer operating at 800 MHz (^{1}H frequency) equipped with a TCI cryoprobe.

Infrared spectroscopy: IR was conducted with solid samples on a Perkin Elmer Spectrum 100 FT-IR Spectrometer using a universal ATR sampling accessory.

Mass spectrometry (MS): Reaction monitoring with mass spectrometry was conducted on a Waters ZQ Quadruple MS operating in positive ElectroSpray Ionization (ESI) mode and LC-MS results were acquired on an Agilent HP1100 HPLC system coupled to photodiode array detector and a Thermo LCQ-DECA ion-trap MS operating in positive ESI mode. The high-resolution mass spectrometry data used to confirm elemental composition were obtained on a Thermo Scientific Exactive operating in positive ESI mode.

High Performance Liquid Chromatography (HPLC): Analytical and semi-preparative HPLC utilized an Agilent 1200 LC with in-line ultraviolet detection (220 nm, 240 nm or 254 nm). Analytical reversed-phase HPLC used an Agilent Eclipse XDB C_{18} 5 µm 4.6 × 150 mm column and the mobile phases (A = H_2O 0.1% trifluoroacetic acid (TFA), B = acetonitrile 0.1% TFA). 1 mL/min with the following gradient: 0-5 minutes 98% A, 5-20 minutes 2-98% B, 20-25 minutes 98% B, 25-30 minutes 98% A. Semi-preparative reversed-phase HPLC was conducted using an Agilent Eclipse XDB C_{18} 5 µm 21.2 × 150 mm column with the concentration of mobile phase B increasing at a rate of 1%/min (A = H_2O with 0.2% TFA, B = acetonitrile with 0.2% TFA, starting from 100% A at time 0; flow rate, 3 mL/min).

Synthesis

Compound 14 ($Glu(tBu)_2$-C(O)-$Glu(tBu)_2$)

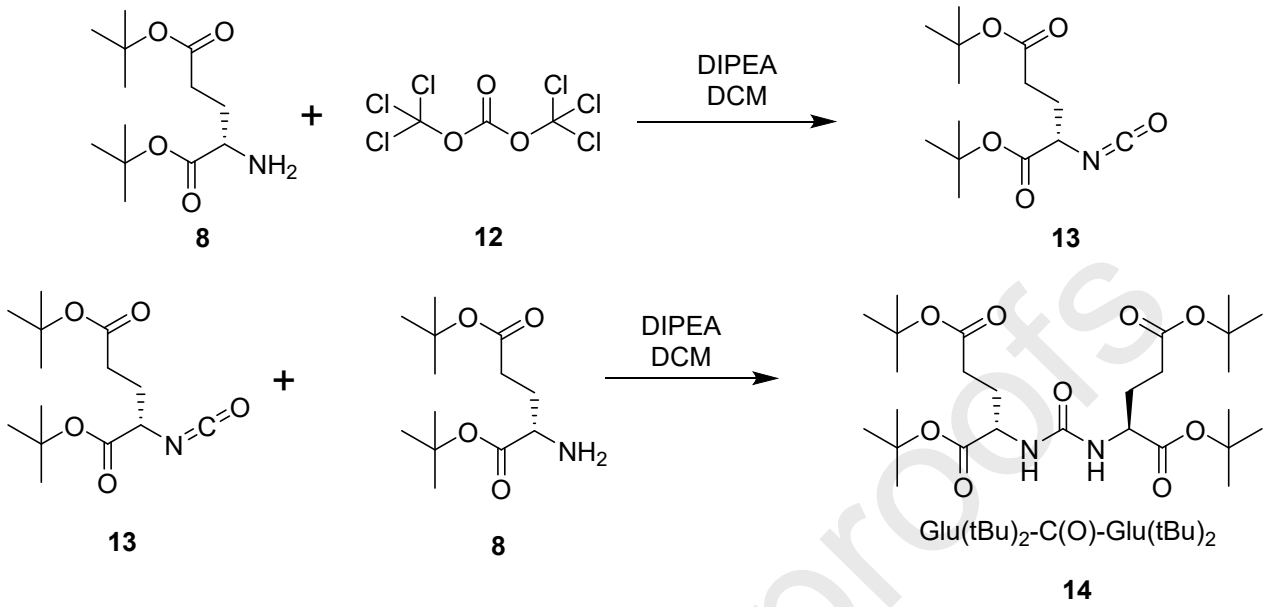

Reaction Scheme 1: Synthesis route for the production of compound **14** ($Glu(tBu)_2$-C(O)-$Glu(tBu)_2$).

An oven-dried three-necked round-bottomed flask with a dropping funnel was attached to a Schlenk line and cycled with vacuum and nitrogen gas three times. Triphosgene (compound **12,** 0.53 mmol, 156 mg, molecular weight (MW) 296.75) was added to the flask which was then cooled to 0°C in an ice bath. L-glutamic acid di-tert-butyl ester (compound **8**, 1.6 mmol, 459 mg, HCl salt, MW 295.8) was dissolved in 20 mL anhydrous dichloromethane (DCM) containing two equivalents of *N*,*N*-Diisopropylethylamine (DIPEA) (550 µL, 3.2 mmol, MW 129.2, density 0.742 g/mL). This solution was added dropwise to the reaction flask over 45 minutes using the dropping funnel, under nitrogen. The solution was stirred throughout addition and some fuming occurred. The ice bath was then removed and the reaction mixture left to warm to room temperature for 1 hour. Then a further 600 mg L-glutamic acid di-tert-butyl ester (compound **8,** 2 mmol, HCl salt, MW 295.8) dissolved in 20 mL of DCM and 600 µL DIPEA (3.5 mmol, MW 129.2, density 0.742 g/mL) was added to the dropping funnel and added slowly to the flask over 45 minutes. The flask remained under nitrogen for 30 minutes post-addition and was then sealed and left to stir overnight. The next day the reaction mixture was washed with water (50 mL x 3) and brine (50 mL x 1), dried over magnesium sulfate and the solvent removed by rotary evaporation. The product, compound **14**, was identified using silica gel TLC with 80:20 DCM:ethyl acetate (starting material R_F = 0, product R_F = 0.65). The crude product was purified using flash chromatography (Biotage Isolaera™ Four) using a 10 g KP SNAP silica column with a DCM and ethyl acetate gradient (100% DCM to 60% DCM, 40% ethyl acetate) and then dried under vacuum to produce compound **14** ($Glu(tBu)_2$-C(O)-$Glu(tBu)_2$) as a white solid (562 mg, 1.03 mmol (MW = 544.69), yield 64%). ^{1}H NMR: ($CDCl_3$, 400 MHz, normalized to chloroform solvent peak[1]): δ 1.39 (s, 18H), 1.42 (s, 18H), 1.83 (m, 2H), 2.02 (m, 2H), 2.27 (m, 4H), 4.30 (dd, *J*= 6.8, 12, 2H), 5.25 (broad s, 2H). ^{13}C NMR: ($CDCl_3$, 100 MHz, normalized to chloroform solvent peak[1]): δ 28.07 (s, 6C), 28.14 (s, 6C), 28.52 (s, 2C), 31.64 (s, 2C), 53.13 (s, 2C), 80.53 (s, 2C), 82.03 (s, 2C) 156.94 (s, 1C) 172.13 (s, 2C), 172.50 (s, 2C). High-resolution mass spectrometry: $[C_{27}H_{48}N_2O_9+H]^+$: observed m/z 545.3426, theoretical m/z 545.3433,$[C_{27}H_{48}N_2O_9+Na]^+$: observed m/z 567.3241, theoretical m/z 567.3252.

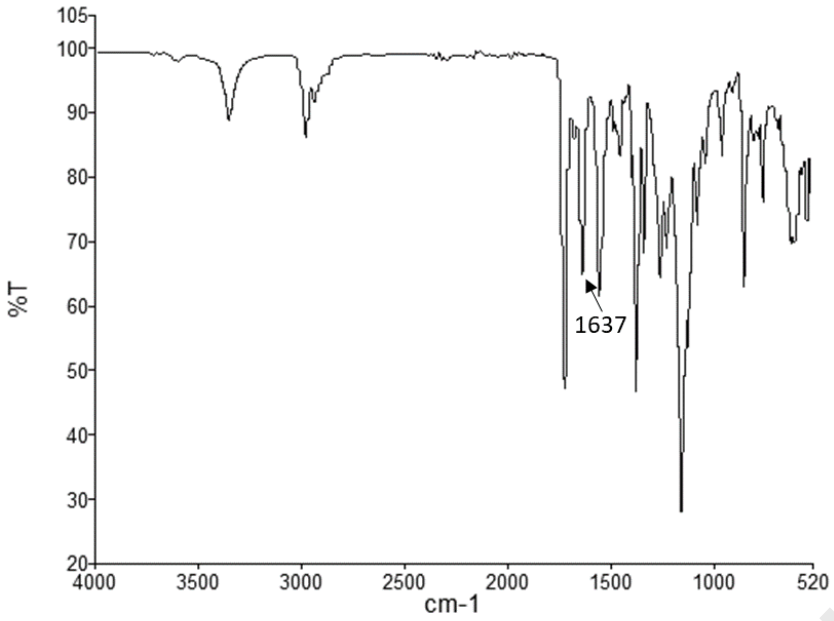

Figure 1: IR spectrum for compound **14** ($Glu(tBu)_2$-C(O)-$Glu(tBu)_2$) : a characteristic urea C=O stretch is seen at 1637 cm^{-1}.[2]

Compound 5 (Glu-C(O)-Glu)

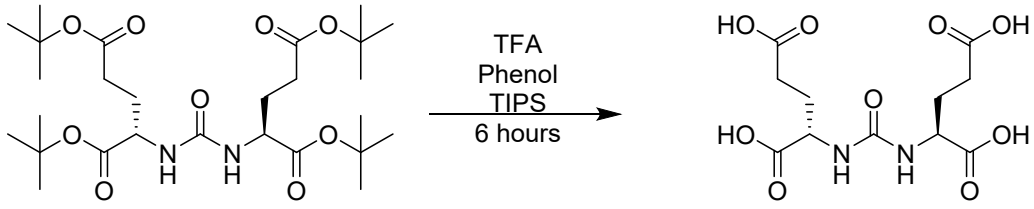

14 Glu-C(O)-Glu **5**

Reaction scheme 2: Synthesis route for the production of compound **5** (Glu-C(O)-Glu).

A solution containing 75 mg phenol (0.8 mmol, MW 94.11), 75 µL H_2O, 35.5 µL TIPS (0.17 mmol, MW 158.36, density 0.773 g/mL) and 1.5 mL TFA (19.6 mmol, MW 114.02, density 1.489 g/mL) was added to 66 mg of $Glu(tBu)_2$-C(O)-$Glu(tBu)_2$ (compound **14** 0.12 mmol, MW = 544.69) and the mixture stirred at room temperature for 6 hours. After this time 5 mL DCM was added and then the solution was evaporated to ~0.5 mL under a stream of nitrogen gas, and 15 mL of ice-cold diethyl ether was added, whereupon a white solid precipitated. The solid was separated from the diethyl ether by centrifugation, dried overnight at room temperature, dissolved in 7 mL water containing 0.1% TFA and then purified by semi-preparative HPLC. The purified sample was freeze-dried, forming a white solid. 18.6 mg (48% yield) of compound **5** (Glu-C(O)-Glu, 50 µmol, MW 320.25) was produced. ^{1}H NMR: (D_2O, 400 MHz, normalized to acetonitrile solvent peak[1]) δ 1.97 (m, 2H), 2.16 (m, 2H), 2.50 (t, *J* = 7.6, 4H), 4.26 (dd, *J* = 5.2, 9.2, 2H). Solvent: 2.06 ppm – acetonitrile, 4.77 ppm – H_2O. ^{13}C NMR: (D_2O plus drop of MeOD, 100 MHz, normalized to methanol solvent peak[1]) δ 27.82 (s, 2C), 31.50 (s, 2C), 160.65 (s, 1C), 177.60 (s, 2C), 178.57 (s, 2C). High-resolution mass spectrometry: $[C_{11}H_{16}N_2O_9+H]^+$: observed m/z 321.0924, theoretical m/z 321.0929, $[C_{11}H_{16}N_2O_9+Na]^+$: observed m/z 343.0743, theoretical m/z 343.0748.

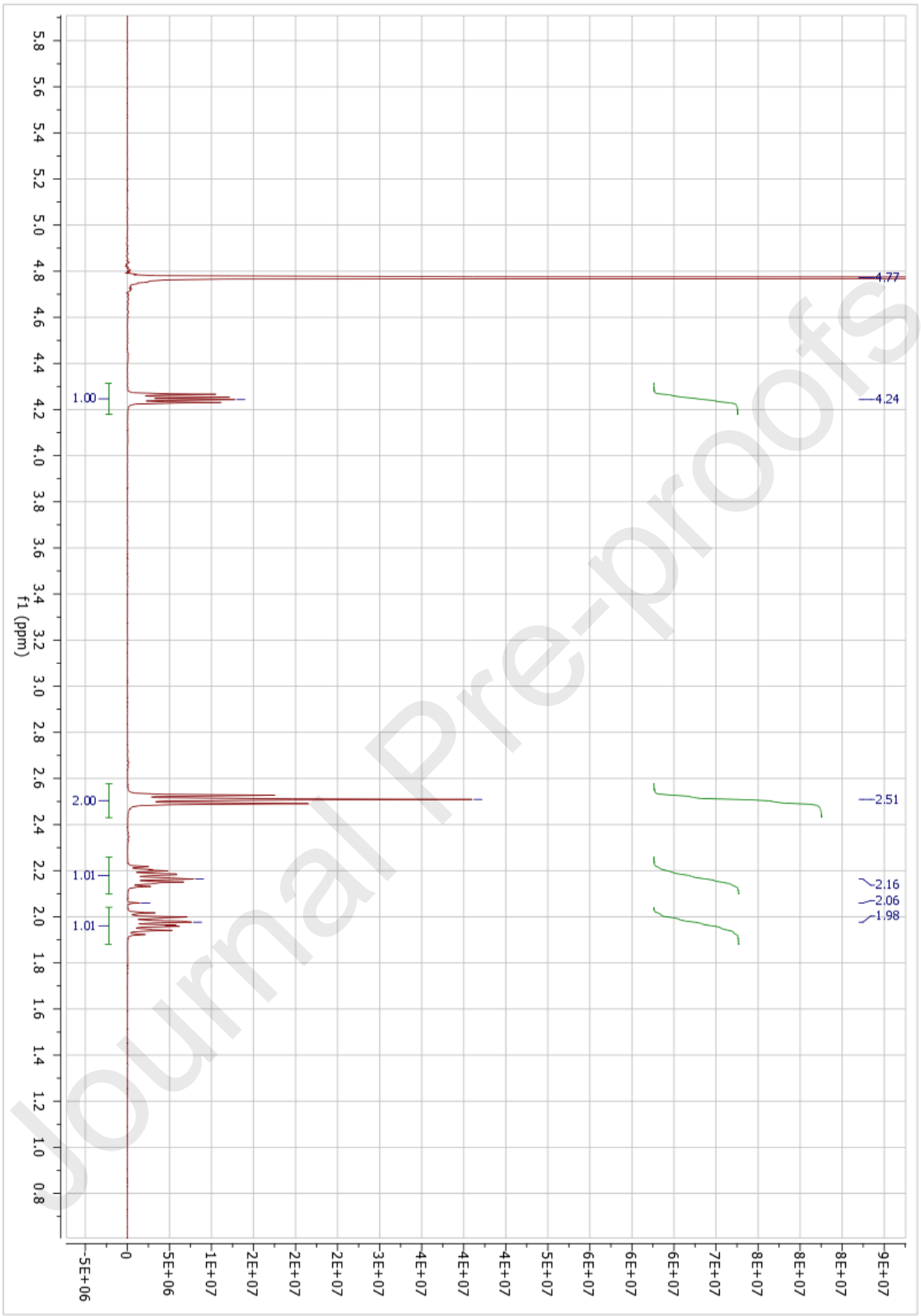

Figure 2: Compound **5** (Glu-C(O)-Glu) ^{1}H NMR: (D_2O, 400 MHz, normalized to acetonitrile solvent peak[1]) δ 1.97 (m, 2H), 2.16 (m, 2H), 2.50 (t, *J* = 7.6, 4H), 4.26 (dd, *J* = 5.2, 9.2, 2H). Solvent: 2.06 ppm – acetonitrile, 4.77 ppm – H_2O. No other impurities detected.

Compound 10 ($Glu(tBu)_2$-C(S)-$Glu(tBu)_2$)

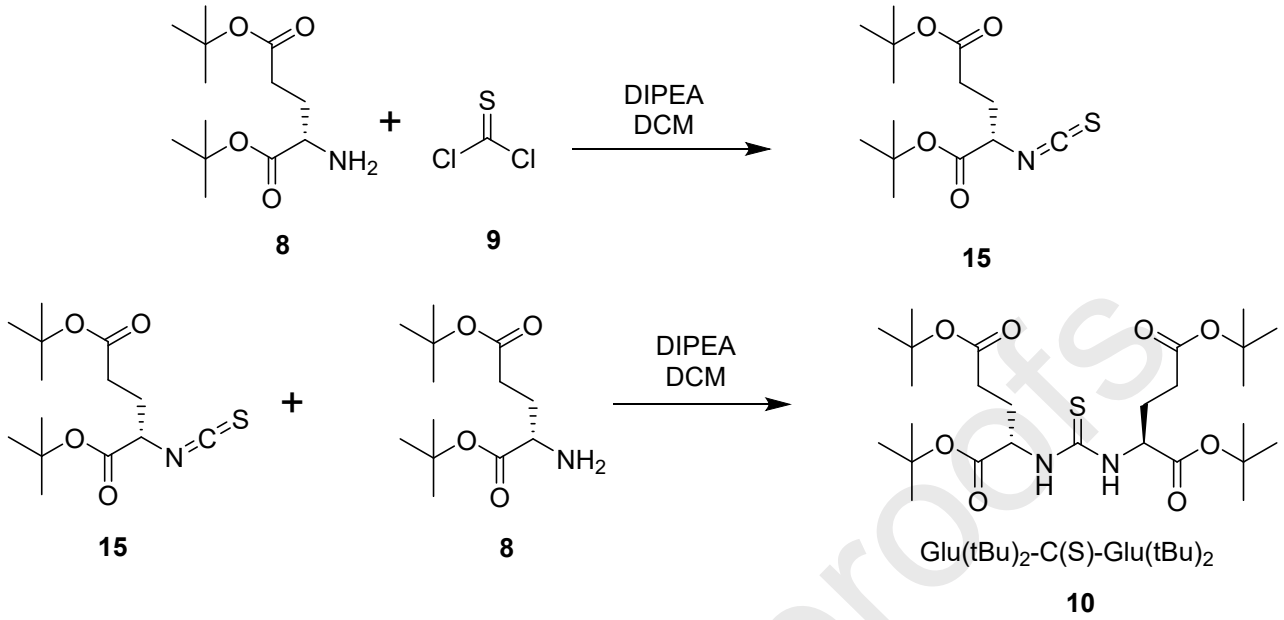

Reaction Scheme 3: Synthesis route for the production of compound **10** ($Glu(tBu)_2$-C(S)-$Glu(tBu)_2$).

An oven-dried three-necked round-bottomed flask with a dropping funnel was attached to a Schlenk line and cycled with vacuum and nitrogen gas three times. 5 mL DCM was added to the round-bottomed flask, followed by 260 µL of thiophosgene (compound **9**, 3.4 mmol, MW 114.98, density 1.5, bright orange liquid). The flask was then cooled to 0°C in an ice bath. L-glutamic acid di-tert-butyl ester (compound **8**, 1 g, 3.4 mmol, HCl salt, MW 295.8) was dissolved in 20 mL anhydrous DCM and 1.1 mL DIPEA (6.3 mmol, MW 129.2, density 0.742 g/mL) was added dropwise to the flask over 45 minutes using the dropping funnel whilst the flask remained under nitrogen. The solution was stirred throughout the addition and some fuming occurred. The ice bath was then removed and the reaction mixture was left to warm to room temperature for 1 hour. Then a further 1.1 g L-glutamic acid di-tert-butyl ester (compound **8**, 3.7 mmol, HCl salt, MW 295.8) dissolved in 20 mL of DCM and 1.1 mL DIPEA (6.3 mmol, MW 129.2, density 0.742 g/mL) was added dropwise to the flask over 45 minutes using the dropping funnel. The flask was left under nitrogen for a further 30 minutes, then sealed and left to stir overnight. The next day the reaction mixture was washed with water (50 mL x 3) and brine (50 mL x 1), dried over magnesium sulfate and then the solvent removed by rotary evaporation. The product compound **10** was identified using silica TLC with 95:5 DCM:ethyl acetate (starting material R_F = 0, product R_F = 0.4). The crude product was purified using flash chromatography (Biotage Isolaera™ Four) using a 25 g SNAP KP silica column with a DCM and ethyl acetate gradient (100% DCM to 90% DCM, 10% ethyl acetate) and then dried under vacuum to produce compound **10** ($Glu(tBu)_2$-C(S)-$Glu(tBu)_2$)as a light yellow oil which solidified upon standing. 260 mg, 0.46 mmol, a 14% yield (MW 560.75). ^{1}H NMR: ($CDCl_3$, 400 MHz, normalized to chloroform solvent peak [1]): δ 1.41 (s, 18H), 1.43 (s, 18H), 1.98 (m, 2H), 2.09 (m, 2H), 2.31 (m, 4H), 4.84 (broad s, 2H), 6.79 (broad s, 2H). ^{13}C NMR: ($CDCl_3$, 100 MHz, normalised to chloroform solvent peak [1]): δ 27.75 (s, 2C), 28.06 (s, 6C), 28.13 (s, 6C), 31.39 (s, 2C), 56.93 (s, 2C), 80.84 (s, 2C), 82.53 (s, 2C) 171.38 (s, 2C) 172.51 (s, 2C), 182.50 (s, 1C). High-resolution mass spectrometry: $[C_{27}H_{48}N_2O_8S+H]^+$: observed m/z 561.3195, theoretical m/z 561.3204, $[C_{27}H_{48}N_2O_8S+Na]^+$: observed m/z 583.3010, theoretical m/z 583.3024

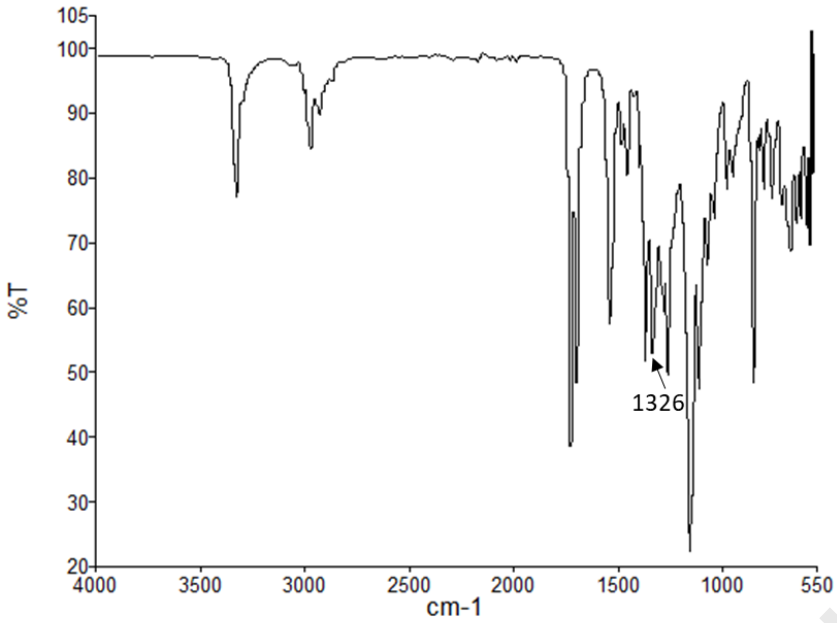

Figure 3: IR spectrum for compound **10** ($Glu(tBu)_2$-C(S)-$Glu(tBu)_2$) : a characteristic thiourea C=S stretch is seen at 1326 cm^{-1}.[2]

Compound 6 (Glu-C(S)-Glu)

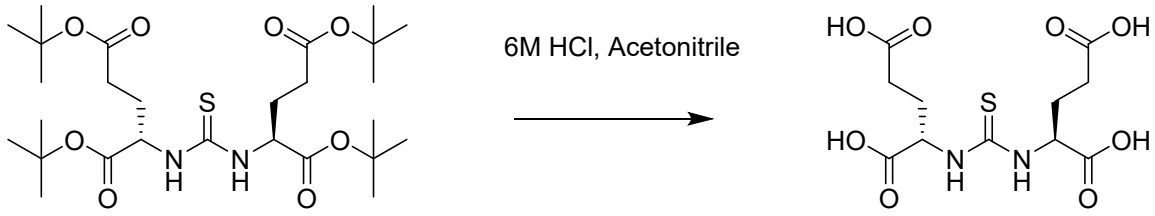

$Glu(tBu)_2$-C(S)-$Glu(tBu)_2$

10

Glu-C(S)-Glu

6

Reaction Scheme 4: Synthesis route for the production of compound **6** ($Glu(tBu)_2$-C(S)-$Glu(tBu)_2$).

$Glu(tBu)_2$-C(S)-$Glu(tBu)_2$ (Compound **10**, 30 mg, 53.5 µmol, MW 560.75) was dissolved in 4 mL acetonitrile and 2 mL 6 M HCl (final concentration 5 mg/mL) and stirred at room temperature for 8 hours. The reaction was monitored by HPLC. Figure 4 shows the HPLC results at the point that the reaction was quenched. After 8 hours the solution was neutralized to pH 3-7 with NaOH (4 M ~3330 µL), frozen and then freeze-dried to form a white powder. The solid was dissolved in 6 mL H_2O containing 0.1% TFA and then purified by semi-preparative HPLC and freeze-dried forming a white solid. Note: our previous studies had shown that compound **6** (Glu-C(S)-Glu) and compound **11** (Glu-C(S)-pyroGlu) could be successfully separated by HPLC (Figure 5). 7.7 mg (43% yield) of compound **6** (Glu-C(S)-Glu, 22.8 µmol, MW 336.32). ^{1}H NMR: ($(CD_3)_2SO$, 400 MHz, normalized to tetramethylsilane solvent peak[1]): δ 1.85 (m, 2H), 2.01 (m, 2H), 2.25 (m, 4H), 4.79 (dd, *J*=7.2, 12.8, 2H), 7.82 (d, *J*=8, 2H), 12.45 (broad s, 4H). Residual solvents and impurities: 0.00 ppm - tetramethylsilane, 2.50 ppm - DMSO, 3.32 ppm - H_2O, 2.67 ppm unidentified impurity which accounts for 6% of signal. ^{1}H NMR: (D_2O PBS, 400 MHz, normalized to acetone solvent peak[1]) δ 2.10 (m, 2H), 2.24 (m, 2H), 2.48 (t, *J*=8 4H), 4.67 (broad 2H). The CH peak at 4.67 ppm is affected by the water suppression. Residual solvent: 2.22 ppm - acetone. High-resolution mass spectrometry: $[C_{11}H_{16}N_2O_8S+H]^+$: observed m/z 337.0697, theoretical m/z 337.0700, $[C_{11}H_{16}N_2O_8S+Na]^+$ observed m/z 359.0515, theoretical m/z 359.0520.

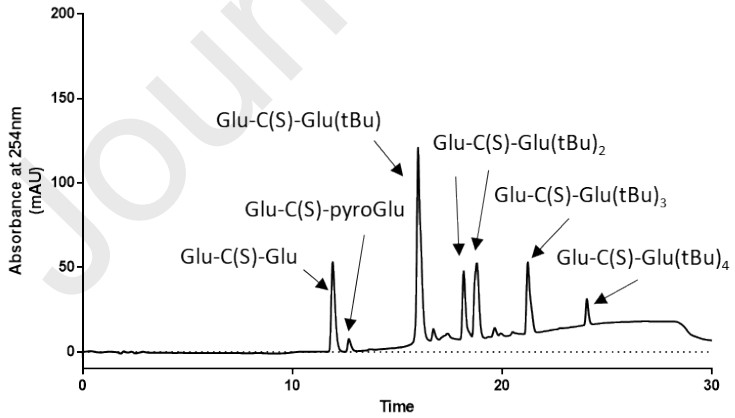

Figure 4: HPLC of reaction mixture compound **10** ($Glu(tBu)_2$-C(S)-$Glu(tBu)_2$)(30 mg, 53.5 µmol, MW 560.75) dissolved in 4 mL acetonitrile and 2 mL 6 M HCl (final concentration 5 mg/mL) after it had been stirred at room temperature for 8 hours. This was the point at which the reaction mixture was quenched.

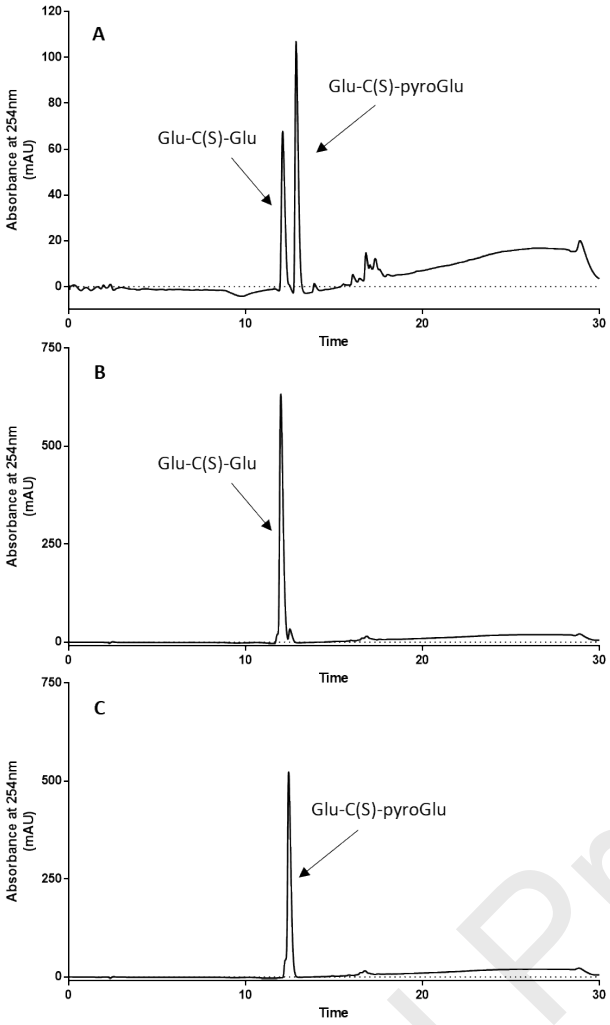

Figure 5: HPLC results to show that compound **6** (Glu-C(S)-Glu) and compound **11** (Glu-C(S)-pyroGlu) could be separated by HPLC in high purity and did not interconvert.

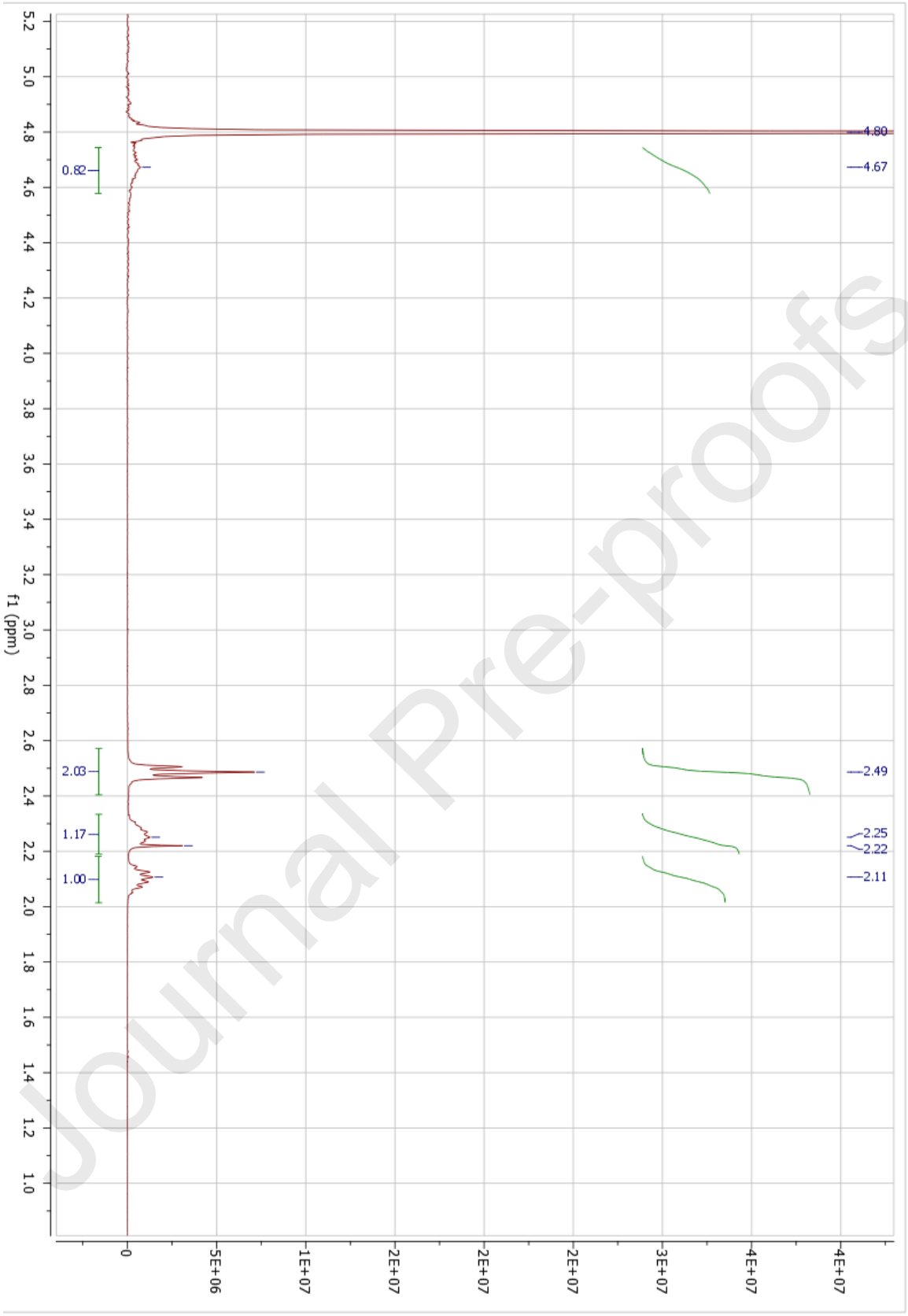

Figure 6: Compound **6** (Glu-C(S)-Glu) ^{1}H NMR: ^{1}H NMR: ((D_2O PBS, 400 MHz, normalized to acetone solvent peak[1]) δ 2.10 (m, 2H), 2.24 (m, 2H), 2.48 (t, *J*=8 4H), 4.67 (broad ~2H). The CH peak at 4.67 ppm is affected by the water suppression. Residual solvent: 2.22 ppm - acetone. No other impurities detectable.

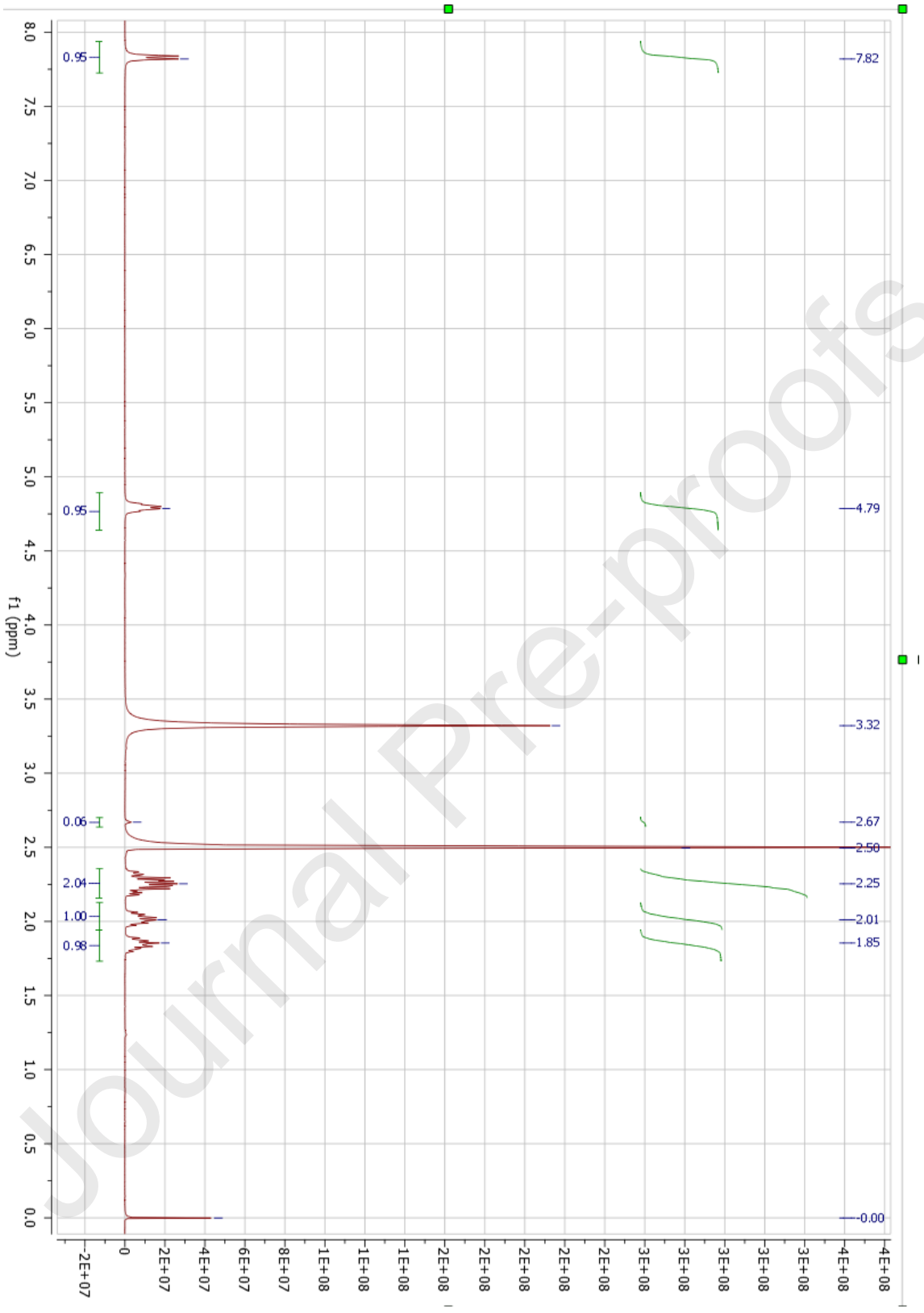

Figure 7: Compound **6** (Glu-C(S)-Glu) ^{1}H NMR: ($(CD_3)_2SO$, 400 MHz, normalized to tetramethylsilane solvent peak[1]): δ 1.85 (m, 2H), 2.01 (m, 2H), 2.25 (m, 4H), 4.79 (dd, *J*=7.2, 12.8, 2H), 7.82 (d, *J*=8, 2H), 12.45 (broad s, 4H). Residual solvents and impurities: 0.00 ppm - tetramethylsilane, 2.50 ppm - DMSO, 3.32 ppm - H_2O, 2.67 ppm unidentified impurity which accounts for 6% of signal.

Quantitative ^{1}H NMR studies.

Quantitative ^{1}H NMR (800 MHz) studies with a repetition time of 20 seconds were conducted to determine the concentrations of the two synthetically prepared inhibitors compounds **5** and **6** with a known concentration of maleic acid as a standard. The signal to noise ratio in the sample was increased through the use of a Bruker Z106898 oval NMR tube which reduces the resistance to radiofrequency penetration when analyzing samples with high salt content[3]. Based on the concentrations determined using these NMR studies, 20 mM solutions of each inhibitor were prepared and used for IC_{50} studies.

NMR stability pH 7

In order to ensure that compound **6** (Glu-C(S)-Glu) was stable at near-neutral pH, the compound was dissolved in D_2O containing ten times the standard concentration of PBS (NaCl 1.37M, KCl 27 mM, Na_2HPO_4 100 mM, KH_2PO_4 18 mM). This only brought the pH to 4 and so ammonium acetate was used to raise the pH to at least 6.5 (final concentration 1 M ammonium acetate). This mixture was then monitored by ^{1}H NMR (400 MHz) at time points up to 48 hours to look for any evidence of cyclisation. The same experiment was also carried out with compound **5** over 48 hours.

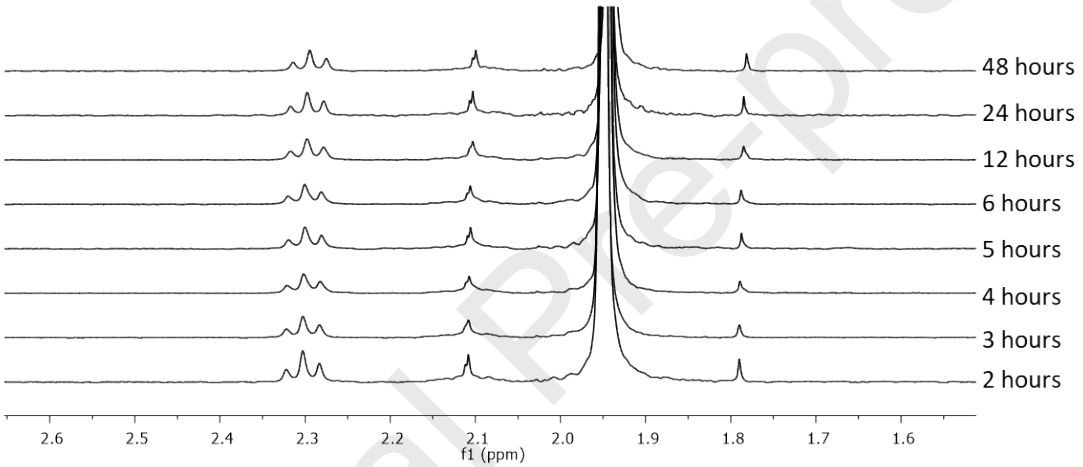

Figure 8: Stability study for compound **6** (Glu-C(S)-Glu) monitored by ^{1}H NMR spectroscopy (400 MHz). No change in the spectra over the time-course confirms the compound is stable under these conditions for up to 48 hours.

Stability in the presence of cells by NMR

Stability of compound **6** (Glu-C(S)-Glu) in the presence of cells: NMR spectroscopy was used to determine if cyclisation of compound **6** to compound **11** occurred whilst the blocking agent was incubated with cells. DU145-PSMA cells (1×10^6 per well) were seeded in a 6-well plate, 1 day before the assay. At the time of the assay, the medium was removed and replaced with 980 µL of PBS at 37°C. Then 20 µL of compound **6** was added (dissolved in 1 M ammonium acetate and 10 x PBS) to give a final concentration of 400 µM on the cells. The cells were then incubated at 37°C for 1 hour. As a control, wells without any cells were incubated with compound **6** in the same way. After 1 hour the supernatant was removed from the wells (containing cells or with no cells), centrifuged to remove any cell debris or particulates, then analyzed by ^{1}H NMR spectroscopy at 400 MHz.

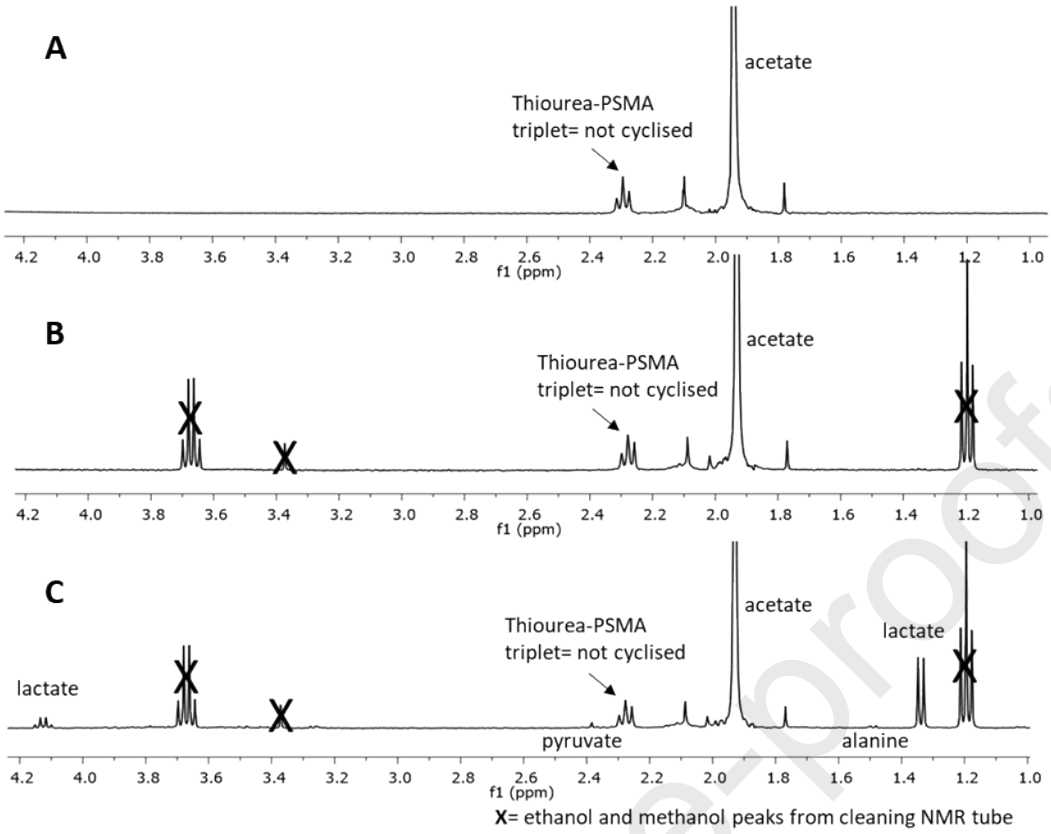

Figure 9: ^{1}H NMR (400 MHz) spectrum of: (A) Solution of compound **6** added to the cells for the IC_{50} assay. The signal at 2.2 ppm is identical to that in the stability study. (B) Compound **6**after incubation at 400 µM in an empty 6 well plate in 1 mL PBS for 1 hour. (C) Compound **6** after incubation at 400 µM with 1 million cells in a 6 well plate in 1 mL PBS for 1 hour. Peaks corresponding to the release of lactic acid, pyruvate and alanine from the cell can be detected, but the signal coming from the thiourea-PSMA at 2.3 ppm does not change showing it is stable under these conditions. Ethanol and methanol residue from NMR tube preparation are marked with a cross.

IC_{50} assay method

The GCP(II)/PSMA-negative cell line chosen was DU145, a human carcinoma prostate cancer cell line derived from a brain metastatic site, which does not express GCP(II)/PSMA. The GCP(II)/PSMA-expressing cell line chosen was a genetically modified daughter cell line of DU145, DU145-PSMA. This cell line had previously been transduced to express full-length human GCP(II)/PSMA, with a published method[4]. These cells were cultured in RPMI 1640 medium supplemented with 10% fetal bovine serum, 2 mM L-glutamine, and penicillin/streptomycin. To prepare for experiments, cells were grown at 37°C in an incubator equilibrated with humidified air and 5% CO_2.

IC_{50}: To determine the IC_{50}, competitive binding studies were performed with DU145-PSMA cells with 1 nM [^{68}Ga]Ga-DOTA-PSMA as the probe and blocking with compounds **5, 6** and **7** over a range of concentrations (1 nM - 400 µM). As both compound **5** and **6** had been dissolved in 10 x PBS and 1 M ammonium acetate to maintain pH at 7 for the stability and quantification NMR studies, care was taken to ensure that the same amount of these reagents were added into every well used in this assay. Cells (0.25×10^6 per well) were seeded in a 24-well plate, 1 day before the assay. At the time of the

assay, the medium was removed and replaced with 240 µL of complete RPMI medium at 37°C. Increasing concentrations of compounds **5, 6** and **7** (5 µL dissolved in 1 M ammonium acetate and 10 x PBS) followed by 1 nM [^{67}Ga]Ga-DOTA-PSMA (5 µL, molar activity 5–10 MBq/nmol, diluted in PBS) were added to the cells (total volume, 250 µL). A control was also included to account for non-specific binding where non-GCP(II)/PSMA-expressing cells (DU145) prepared in the same way were also incubated with 1 nM [^{67}Ga]Ga-DOTA-PSMA. After 1 hour incubation at 37°C, the supernatant was removed and the cells were washed with PBS (2 × 0.25 mL), lysed with NaOH (1 M, 0.25 mL), and the wells washed with PBS (0.25 mL). The activity present in supernatant and lysate was measured by γ-counting. Data were analyzed using GraphPad Prism (version 7.04 GraphPad Software) and a 1-site–fit log IC_{50} algorithm.

Relationship between Ki and IC_{50}

The mathematical relationship between K_i and IC_{50} can be described by the Cheng–Prusoff equation[5]:

$$IC_{50} = K_i\left(1 + \frac{[S]}{K_M}\right)$$

Equation 1: Cheng–Prusoff relationship

Where [S] is the substrate concentration and K_M is the Michaelis constant of the substrate. In certain circumstances IC_{50} values do trend towards K_i values – IC_{50} values approximate K_i when the [S] used in the assay is much lower than K_M.

However, in in this report because cells expressing the protein of interest were used - a high concentration of substrate - the criteria of [S] being lower than K_M was not fulfilled. This explains why the IC_{50} values measured were significantly larger than the K_i values previously reported for compounds **5** and **7**.

However, as long the IC_{50} values of two different inhibitors are measured under the same conditions, with the same concentration of substrate, and the inhibitors have the same mechanism of action (the assumption for the set of inhibitors in this report) then ratios of the two inhibitors IC_{50} values are comparable to ratios of K_i measurements using equation 2 [5].

$$\frac{K_{i,1}}{K_{i,2}} = \frac{IC_{50,1}}{IC_{50,2}}$$

Equation 2:

Where $K_{i,1}$ is the K_i of inhibitor 1, $K_{i,2}$ is the K_i of inhibitor 2, $IC_{50,1}$ is the IC_{50} of inhibitor 1 and $IC_{50,2}$ is the IC_{50} of inhibitor 2. As our experiments meet these criteria, the IC_{50} values we obtained are suitable to compare the relative affinity ratios of the three inhibitors, even though the K_i for compound **6** has not been determined.

References

1. Fulmer GR, Miller AJM, Sherden NH, et al. NMR chemical shifts of trace impurities: common laboratory solvents, organics, and gases in deuterated solvents relevant to the organometallic chemist. *Organometallics*. 2010;29(9):2176-2179. doi 10.1021/om100106e

2. Fleming I, Williams D. *Spectroscopic Methods in Organic Chemistry*.; 2019. doi:10.1007/978-3-

030-18252-6

3. Robosky LC, Reily MD, Avizonis D. Improving NMR sensitivity by use of salt-tolerant cryogenically cooled probes. *Anal Bioanal Chem*. 2007;387(2):529-532. doi:10.1007/s00216-006-0982-4

4. Kampmeier F, Williams JD, Maher J, Mullen GE, Blower PJ. Design and preclinical evaluation of a 99mTc-labelled diabody of mAb J591 for SPECT imaging of prostate-specific membrane antigen (PSMA). *EJNMMI Res*. 2014;4(1):13. doi:10.1186/2191-219X-4-13

5. Kalliokoski T, Kramer C, Vulpetti A, Gedeck P. Comparability of Mixed IC50 Data - A Statistical Analysis. *PLoS One*. 2013;8(4). doi:10.1371/journal.pone.0061007

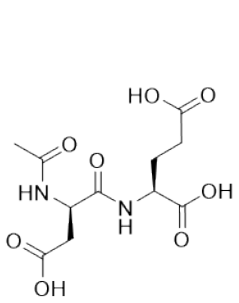

NAAG
1

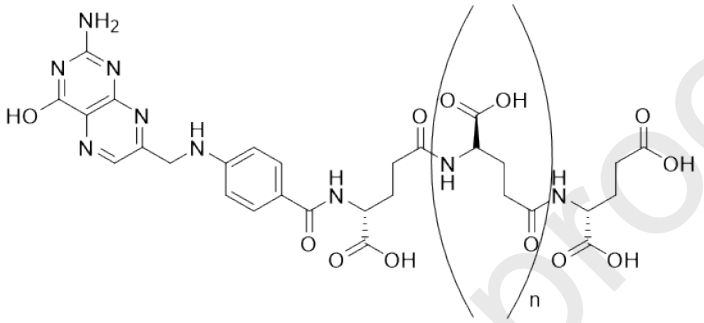

Poly-γ-glutamated-folate
2

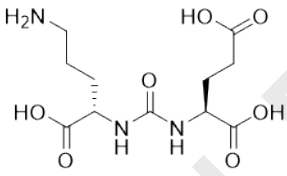

HO-Lys-C(O)-Glu-OH
3

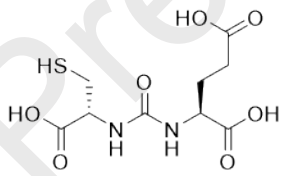

HO-Cys-C(O)-Glu-OH
4

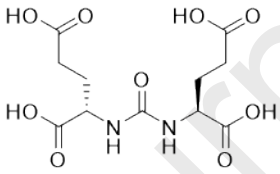

HO-Glu-C(O)-Glu-OH
5

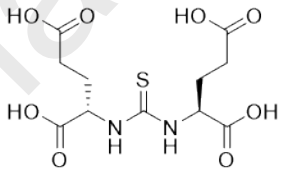

HO-Glu-C(S)-Glu-OH
6

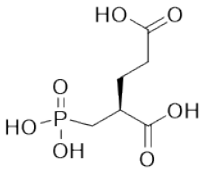

PMPA
7